

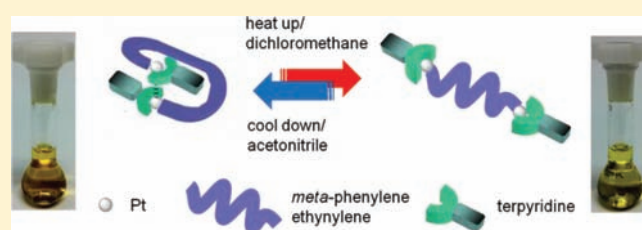
Single-Turn Helix—Coil Strands Stabilized by Metal···Metal and π — π Interactions of the Alkynylplatinum(II) Terpyridyl Moieties in *meta*-Phenylene Ethynylene Foldamers

Sammual Yu-Lut Leung, Anthony Yiu-Yan Tam, Chi-Hang Tao, Hoi Shan Chow, and Vivian Wing-Wah Yam*

Institute of Molecular Functional Materials (Areas of Excellence Scheme, University Grants Committee (Hong Kong)) and Department of Chemistry, The University of Hong Kong, Pokfulam Road, Hong Kong

Supporting Information

ABSTRACT: Dinuclear alkynylplatinum(II) terpyridyl complexes with oligomeric bridge consisting of five repeating *meta*-phenylene ethynylene (*m*PE) units have been found to exhibit a strong tendency to fold back onto themselves to form short helical strands through the stabilization of Pt···Pt and π — π interactions. The steric bulk of the terpyridine ligands and the length of the oligomeric bridge have been found to affect the extent of the intramolecular Pt···Pt interaction that governs the stabilization of the short helical strand in solution. Their folding properties via Pt···Pt and π — π stacking interactions have been studied by ¹H NMR, 2D ROESY NMR, electronic absorption, and emission spectroscopies.



INTRODUCTION

For decades, there has been tremendous interest in designing new classes of luminescent square-planar d⁸ platinum(II) polypyridyl complexes, not only because of their intriguing spectroscopic and luminescence properties,^{1–4} but also their propensity to exhibit metal···metal interaction.^{1a–c,2a–2e,3} Particularly, a class of platinum(II) terpyridyl complexes was shown to exhibit interesting polymorphism in the solid state by forming extended linear chains or dimeric structures which governed the spectroscopic and luminescence properties.^{2,3a} Recently, our group has utilized the intermolecular self-assembly of alkynylplatinum(II) terpyridyl moieties via Pt···Pt and π — π stacking interactions to demonstrate a remarkable color change and luminescence enhancement induced by the presence of polyelectrolytes^{3d–f} and gel formation.^{3g–i} On the other hand, the alkynylplatinum(II) terpyridyl complexes have also been found to aggregate in the presence of single-strand DNA and aptamers with the growth of a characteristic NIR emission.^{3j–l} Apart from the intermolecular self-association, a series of dinuclear platinum(II) terpyridyl complexes, in which the two platinum(II) units are linked through a flexible bridge, have been demonstrated to serve as synthetic organometallic analogues of hairpin DNA.^{3m} Therefore, the alkynylplatinum(II) terpyridyl system is believed to be a versatile moiety in serving as a spectroscopic reporter as well as in providing a control over aggregation properties for the construction of self-assembled architectures.

Recently, there has been a growing interest in the study of polymeric or oligomeric molecular strands that are capable of constructing well-defined secondary conformations in molecular architectures, especially the helix-type in solution.^{5–8} The formation of secondary structures, for instance in proteins and

nucleic acids, can be mimicked by foldamers which have attracted enormous interest in biology and nanosciences.⁵ The process of folding is driven by noncovalent interactions such as hydrogen bonding,⁶ metal coordination,⁷ and π — π stacking interactions.⁸ *meta*-Phenylene ethynylene oligomers are one of the well-known classes of foldamers with six repeating units constituting one turn and that undergo a conformation transition from random coil to helical strand with at least nine aromatic rings stacking together in acetonitrile or at low temperature.^{5b} These molecules can fold back on themselves to enable the favorable π — π interactions to occur between the stacking aromatic repeating units to form a secondary structure.^{5b} Numerous examples demonstrating the utilization of hydrogen bonding and π — π stacking interactions in the stabilization of helical conformations in the organic systems are known.^{5–8} Although works on the utilization of metal—ligand coordination to construct foldamer structures are also known,⁹ unlike their organic counterparts, the reversibility of the folding process is limited due to the presence of the strong metal—ligand interactions. Conversely, the exploitation of metal···metal interactions in stabilizing foldamers in helical conformations has essentially been unexplored. In view of the propensity of the alkynylplatinum(II) terpyridyl system to exhibit reversible intramolecular Pt···Pt and π — π interactions in dinuclear complexes upon introduction of external stimuli,^{3m} it is anticipated that such interaction may provide a driving force for the folding process, or even stabilizing the folded structure in a helical conformation in solutions and serving as a spectroscopic reporter for the probing of folded or unfolded state in the spectroscopic and luminescence study.

Received: September 7, 2011

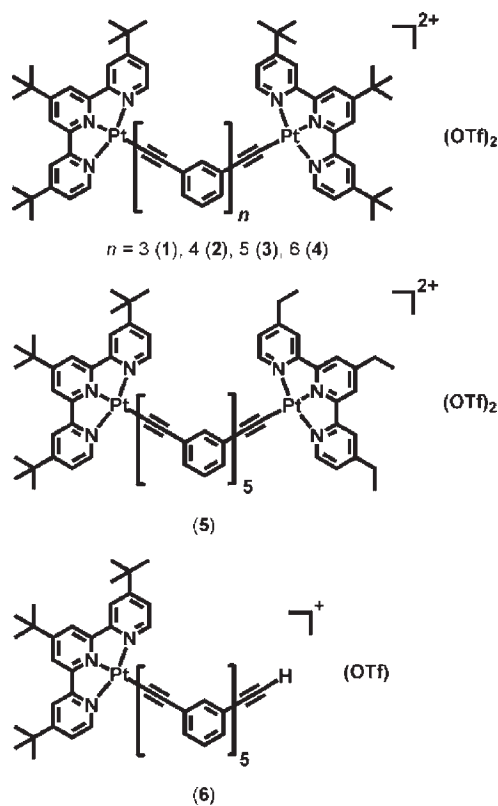
Published: December 20, 2011

Herein, we report a series of dinuclear platinum(II)–containing *meta*-phenylene ethynylene (*m*PE) oligomers of various lengths, end-capped with symmetric or unsymmetric platinum(II) terpyridine units (1–5) (Scheme 1). Their folding properties via Pt···Pt and π – π stacking interactions have been studied by ^1H NMR, 2D ROESY NMR, electronic absorption, and emission spectroscopies. A mononuclear complex (6) with five repeating *m*PE units has also been synthesized for comparison studies.

RESULTS AND DISCUSSION

The syntheses of *m*PE oligomers are based on Sonogashira coupling reactions. Detailed synthetic route for the *m*PE oligomers

Scheme 1. Structures of Dinuclear and Mononuclear Alkynylplatinum(II) Terpyridyl Complexes 1–6



is given in the Supporting Information. The complexes were prepared according to modification of a literature procedure for other related alkynylplatinum(II) terpyridine complexes.^{2d} Complexes 1–4 and 6 were synthesized by reacting the corresponding *meta*-PEs ($\text{H}-(\text{C}\equiv\text{C}-1,3-\text{C}_6\text{H}_4)_n-\text{C}\equiv\text{CH}$, $n = 3-6$) with $[(^t\text{Bu}_3\text{trpy})\text{PtCl}](\text{OTf})$ (molar ratio 1:2 for 1–4, 1:1 for 6) in degassed *N,N*-dimethylformamide containing triethylamine in the presence of a catalytic amount of copper(I) iodide. The unsymmetric dinuclear alkynylplatinum(II) complex 5 was prepared according to the procedure similar to that described for the symmetric species, except 6 and $[(\text{Et}_3\text{trpy})\text{PtCl}](\text{OTf})$ were used in 1:1 molar ratio. The reaction mixture was stirred overnight at room temperature. Chromatography on silica gel using dichloromethane–acetone mixture (10:1 v/v) as eluent, followed by the diffusion of diethyl ether vapor into acetonitrile solution gave 1–6 as yellow to orange solids. All the complexes have been well characterized by ^1H and ^{13}C NMR, IR spectroscopy, FAB mass spectrometry, and elemental analyses.

The ^1H NMR spectra for all the complexes were studied in both CDCl_3 and CD_3CN at 298 K. Interestingly, while all the ^1H NMR spectra showed well-resolved sharp signals with well-defined coupling patterns, the dinuclear complexes with five or six repeating *m*PE units (3–5) in CD_3CN showed signals that are unusually upfield-shifted from those in CDCl_3 , suggesting the presence of molecular association in CD_3CN . The ^1H NMR spectra were found to be independent of concentration within the concentration range of 10^{-3} – 10^{-5} M, suggestive of molecular association that is intramolecular in nature. Variable-temperature ^1H NMR experiments were then performed, which showed that the dinuclear complexes with five or six repeating *m*PE units (3–5) displayed upfield-shifted terpyridine proton signals upon a decrease in temperature in CD_3CN (Supporting Information Figures S1–S3). Solvent titration experiments on 3 (Figure 1) also showed that in general, starting from 30% CD_3CN onward, the proton signals on both phenyl rings and terpyridines became significantly upfield shifted. The upfield shifts observed in the NMR spectra upon decreasing the temperature or switching to a more polar solvent are attributed to π – π stacking interactions between the platinum(II) terpyridyl moieties themselves. Similar upfield shifts have also been found in other related systems.^{3m,n,8j} In addition to the 1D NMR experiment, the protons of the 4'- and 4'''-*tert*-butyl groups on the terpyridines displayed strong NOE signals with the phenyl

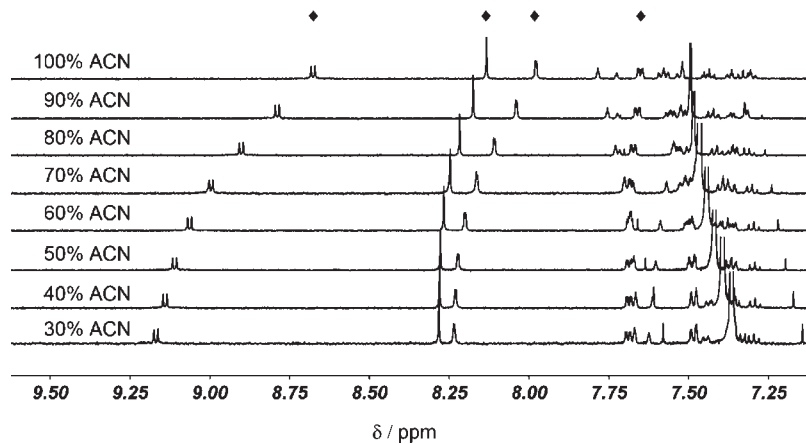


Figure 1. ^1H NMR spectral traces at different compositions of CD_3CN in CDCl_3 for 3 (5×10^{-5} M, 500 MHz, 298 K). Proton signals correspond to the terpyridyl moiety (♦).

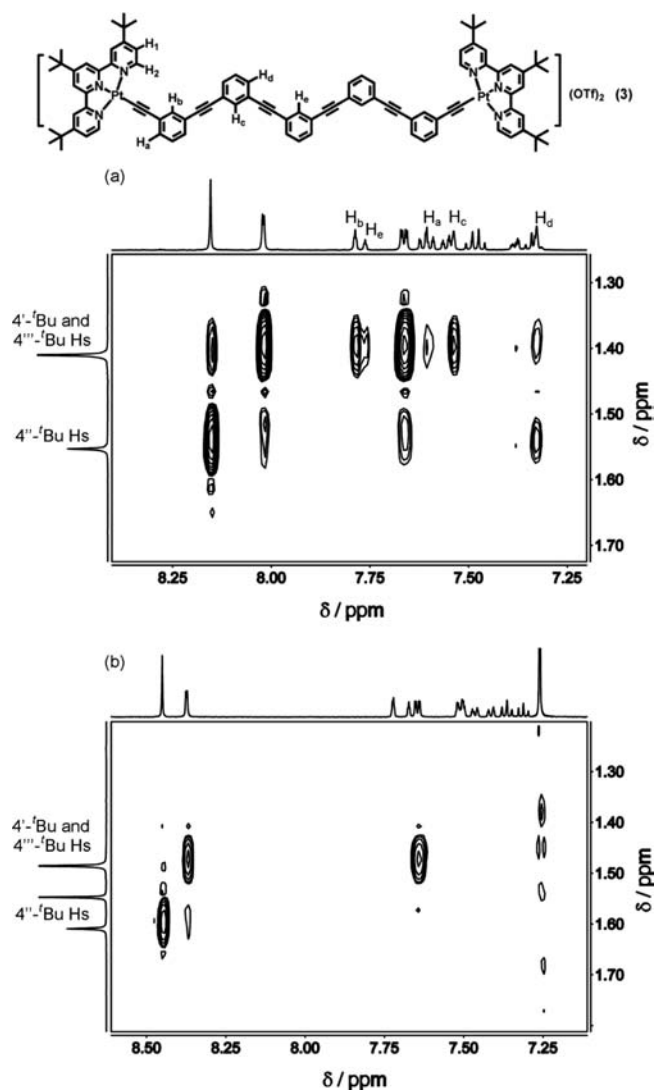


Figure 2. (a) Partial ^1H – ^1H ROESY spectrum of **3** (3×10^{-4} M, 500 MHz, 298 K) for the *tert*-butyl groups on terpyridine and aryl region in CD_3CN . (b) Partial ^1H – ^1H ROESY spectrum of **3** (7×10^{-4} M, 500 MHz, 298 K) for the *tert*-butyl groups on terpyridine and aryl region in CDCl_3 .

rings on *mPE* in the 2D ROESY NMR spectrum of **3** in CD_3CN as shown in Figure 2a, with a distance of 3.14–3.82 Å¹⁰ estimated from the integrals of the cross-peaks. This suggested that the platinum(II) terpyridyl moieties would have a close proximity with the phenyl rings to self-assemble in acetonitrile. On the contrary, these NOE signals were absent in CDCl_3 , in which the molecules adopted a random coil conformation with the two platinum(II) terpyridyl moieties being far away from each other (Figure 2b). Therefore, it is suggested that there is a conformational change for the complexes with five or six repeating units under different solvent and temperature environments.

In the UV–vis absorption study, complexes **1**–**6** gave pale yellow solutions in CH_2Cl_2 with the intense intraligand (IL) [$\pi \rightarrow \pi^*$] transitions of the terpyridyl and alkynyl ligands at 302–340 nm and the low-energy absorptions at 412–470 nm assigned as metal-to-ligand charge-transfer (MLCT) [$d\pi(\text{Pt}) \rightarrow \pi^*(\text{tpy})$] transitions mixed with alkynyl-to-terpyridine ligand-to-ligand charge transfer (LLCT) [$\pi(\text{C}\equiv\text{C}) \rightarrow \pi^*(\text{tpy})$] character.

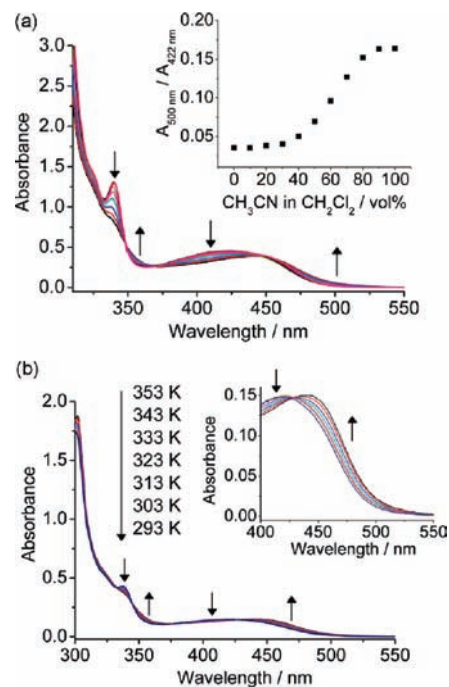


Figure 3. (a) UV–vis absorption spectral traces of **3** in CH_2Cl_2 (6.0×10^{-5} M) with increasing CH_3CN content at 298 K. The inset shows the absorbance ratio $A_{500\text{ nm}}/A_{422\text{ nm}}$ as a function of solvent compositions. (b) UV–vis spectra of **3** (4.6×10^{-5} M) in CH_3CN with decreasing temperature from 353 to 293 K. The inset shows the expansion of the UV–vis absorption spectra in the 430–550 nm region.

However, upon increasing the CH_3CN content in CH_2Cl_2 , the dinuclear complex **3** with *mPE* pentamer showed a decrease in the intraligand [$\pi \rightarrow \pi^*$ (alkynyl)] absorption band at 338 nm and the appearance of an absorption tail at 500 nm (Figure 3a), whereas the mononuclear complex **6** did not show such a change but instead showed a typical negative solvatochromism^{4b} at 480 nm in CH_3CN under similar dilute concentrations (10^{-5} M) (Figure S4). To further investigate the differences in the absorption behavior of the di- and mononuclear platinum complexes, variable-temperature UV–vis absorption spectroscopy on **3** and **6** was performed. Upon decreasing the temperature from 353 to 293 K in CH_3CN , the UV–vis spectrum of **3** showed an increase in the low-energy absorption tail (Figure 3b), similar to the observation of increasing the polarity of the solvent with increasing acetonitrile content, while temperature has a negligible effect on the UV–vis spectrum of **6** under such dilute concentration conditions. Furthermore, the absorbance drop of the high-energy absorption band at 338 nm is indicative of a configuration transformation of the *mPE* units from the *transoid* to the *cisoid* form, similar to that reported by Moore and co-workers.^{5b,8a,8b,8g,8h} The UV–vis absorption traces of **3** (3.0×10^{-5} M) in CH_2Cl_2 with increasing CH_3CN content ranging from 250 to 550 nm are shown in Figure S5. These, together with the appearance of the low-energy absorption tail typical of metal–metal-to-ligand charge-transfer (MMLCT) transition, as well as the good agreement with Beer’s law in the concentration range of 5.94×10^{-6} to 7.43×10^{-4} M for **3** in CH_3CN (Figure S6), are suggestive of molecular self-assembly that leads to the intramolecular self-assembly of the two terminal platinum(II) terpyridyl moieties to form a single-turn helical strand. A plot of $A_{500\text{ nm}}/A_{422\text{ nm}}$ against % CH_3CN in CH_2Cl_2 showed a sigmoidal curve, supportive of cooperative folding

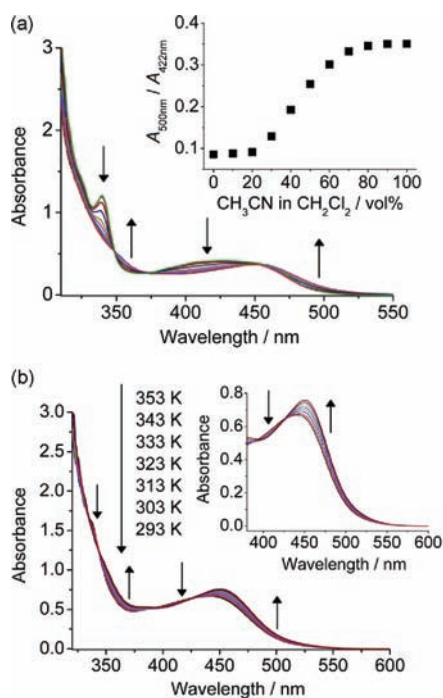


Figure 4. (a) UV-vis absorption spectral traces of **5** in CH_2Cl_2 (3.3×10^{-5} M) with increasing CH_3CN content at 298 K. The inset shows the absorbance ratio $A_{500\text{nm}}/A_{422\text{nm}}$ as a function of solvent compositions. (b) UV-vis spectra of **5** (6.6×10^{-5} M) in CD_3CN with decreasing temperature from 353 to 293 K. The inset shows the expansion of the UV-vis absorption spectra in the 430–550 nm region.

(Figure 3a, inset).^{5b,8a,8b,8g,8h} A helix stabilization energy $\Delta G(\text{CH}_3\text{CN})$ of $-2.3 \text{ kcal mol}^{-1}$ was obtained for **3** in CH_3CN . Detailed calculation of the helix stabilization energy (ΔG) for **3–5** is given in the Supporting Information.

For **1** and **2** with shorter *m*PE units ($n = 3, 4$), only negative solvatochromism was observed for the MLCT transition in CH_3CN (Figure S7), consistent with the shorter length of the *m*PE oligomers that would not allow the two terminal platinum(II) terpyridyl moieties to construct a turn. However, when increasing the repeating units to six ($n = 6$), **4** exhibited similar trends as **3** upon increasing the CH_3CN content or decreasing the temperature in CH_3CN (Figure S8) but with a less negative $\Delta G(\text{CH}_3\text{CN})$ of $-1.2 \text{ kcal mol}^{-1}$. This less favorable ΔG value is probably associated with the misalignment of the two terminal platinum(II) terpyridyl units for the flexible *m*PE hexamer to construct a turn to form a less stable helical strand due to one more repeating unit added.

More interestingly, **5** with one of the ^tBu₃terpy ligands replaced by the less sterically bulky triethyl-substituted terpyridine ligand exhibited a more dramatic increase in the MMLCT absorption tail upon increasing the acetonitrile content (Figure 4a) or decreasing the temperature (Figure 4b). The drop of the high-energy absorption band upon increasing acetonitrile content for **5** (3.6×10^{-5} M) is shown in Figure S9. A more negative $\Delta G(\text{CH}_3\text{CN})$ of $-3.3 \text{ kcal mol}^{-1}$ was obtained for **5**, indicating that the variation in the steric bulk on the terpyridine ligands would alter the extent of the intramolecular Pt···Pt interaction that governs the stabilization of the short helical strand in solution. Similar to complex **3**, both complexes **4** and **5** exhibited absorption bands at 510 nm that obey Beer's law within the

Table 1. A Summary of $\Delta G(\text{pure CH}_3\text{CN})$ for Complexes **3–5**

complexes	$\Delta G/\text{kcal mol}^{-1}$
3	-2.3 ± 0.1
4	-1.2 ± 0.2
5	-3.3 ± 0.2

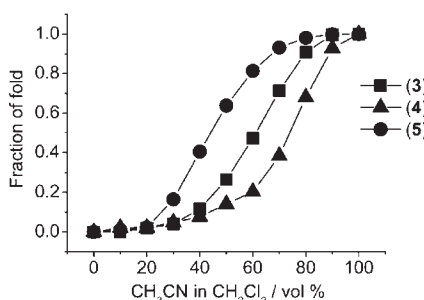


Figure 5. Fraction of fold against percentage of CH_3CN in CH_2Cl_2 for **3–5**.

concentration range of 10^{-6} to 10^{-4} M, disfavoring the possible involvement of an association that is intermolecular in nature. The $\Delta G(\text{CH}_3\text{CN})$ values of **3–5** are summarized in Table 1 and the plots of the fraction of fold versus solvent composition for **3–5** are shown in Figure 5.

In CH_2Cl_2 at 298 K, emission bands of **1–6** at 577–582 nm were observed upon excitation at $\lambda > 400$ nm, which are assigned as an excited state of predominantly ³MLCT/³LLCT character. Interestingly, upon increasing the CH_3CN content, complex **3** showed a growth of a low-energy emission band at 685 nm typical of a ³MMLCT emission with the diminution of the ³MLCT/³LLCT emission typical of the monomeric alkynyl-platinum(II) terpyridine system (Figure 6a). The emission spectral changes of **3** without normalization are shown in Figure S10 to show the quenching effect of the solvent. Similar observation was also found for **4** and **5** (Figures S11 and 6b) upon increasing the acetonitrile content. It is interesting to note that **4** with a *m*PE hexamer showed incomplete switching-off of the monomeric ³MLCT/³LLCT emission even in CH_3CN (Figure 7), in accordance with the proposition that the *m*PE hexamer would form a less stable helical strand due to the misalignment of the terminal platinum(II) terpyridyl moieties. Interestingly, the low-energy ³MMLCT emission band in **3–5** remained even when the concentration was decreased from 10^{-4} M to concentrations as dilute as 10^{-7} M, confirming the involvement of an intramolecular association. On the contrary, the emission maxima of **1, 2**, and **6** showed only a slight blue shift relative to those observed in CH_2Cl_2 (Figure S12) due to the negative solvatochromism,^{4b} with no formation of ³MMLCT emission bands and hence no formation of helical strands. The lack of ³MMLCT emission of **1, 2**, and **6** in the same concentration range of 10^{-6} to 10^{-4} M as those of **3–5** is further supportive of the lack of involvement of intermolecular interactions, which is typically found for *tert*-butyl substituted terpyridyl platinum(II) complexes.^{3a,d,n,4a} The fact that ³MMLCT emission is observable in **3–5**, especially in **3** and **4** with both ligands being ^tBu₃terpy, is possibly a result of the tethering together of the two Pt-^tBu₃terpy units via *m*PE linkers of the appropriate chain length that aided the bringing together of the two end-groups into close

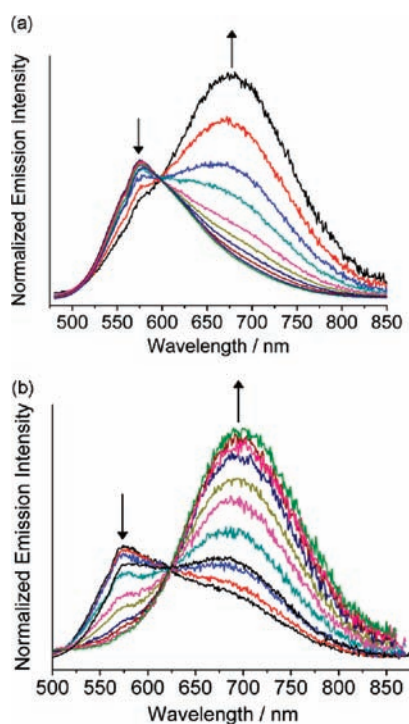


Figure 6. (a) Normalized emission spectral traces at 596 nm for **3** in CH₃CN–CH₂Cl₂ mixtures, 0–100% (6.0×10^{-5} M) upon increasing the CH₃CN fraction. Excitation wavelength = 447 nm. (b) Normalized emission spectral traces at 624 nm for **5** in CH₃CN–CH₂Cl₂ mixtures, 0–100% (3.3×10^{-5} M) upon increasing the CH₃CN fraction. Excitation wavelength = 454 nm.

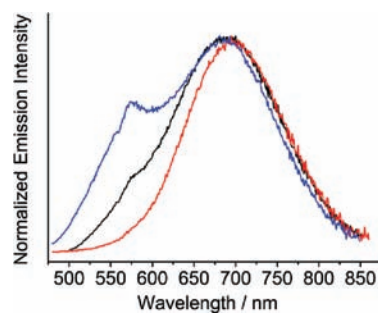


Figure 7. Emission spectra of in CH₃CN for **3** (black), **4** (blue), and **5** (red) at 298 K.

proximity for Pt···Pt and π – π interactions to occur.¹¹ It is likely that such intramolecular Pt···Pt and π – π interactions would also help to stabilize these short helical strands in a cooperative and synergistic manner. In the variable-temperature luminescence study, upon decreasing the temperature, a decrease in monomeric ³MLCT/³LLCT emission and a growth of the ³MMLCT emission were observed in **3** and **4** (Figure 8a and Figure S13), whereas **5** showed a red shift in the ³MMLCT emission with no signs of any monomeric ³MLCT/³LLCT emission bands in CH₃CN even at high temperature (Figure 8b). These, together with the helix stabilization energy obtained from the UV–vis absorption study and the observation that **5** showed the lowest ³MMLCT emission energy (Figure 7), suggested that **5** would adopt the most stable helical strand stabilized by Pt···Pt and π – π interactions of the platinum(II) terpyridine units even at high temperature in

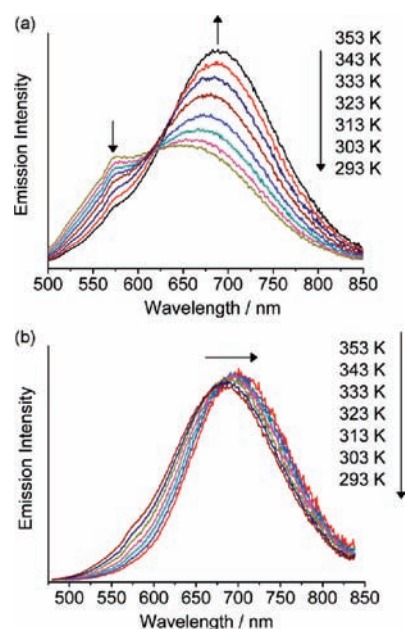


Figure 8. (a) Emission spectra of **3** (6.0×10^{-5} M) with decreasing temperature from 353 to 293 K. Excitation wavelength = 428 nm. (b) Emission spectra of **5** (3.3×10^{-5} M) with decreasing temperature from 353 to 293 K. Excitation wavelength = 427 nm.

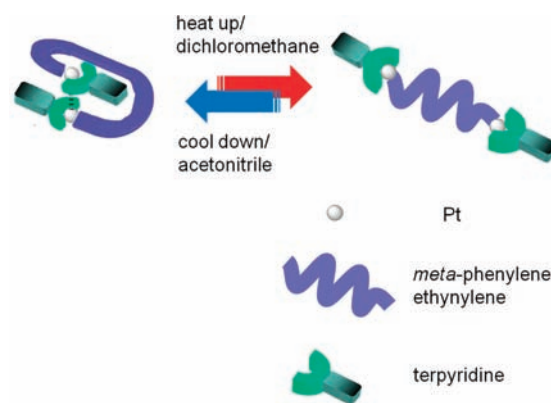


Figure 9. Folding and unfolding of the platinum(II) complexes by temperature and solvent modulation.

CH₃CN. It is also interesting to note that a direct correlation of the extent of Pt···Pt interactions with the stability of the foldamers can be inferred as **5**, with the strongest extent of Pt···Pt and π – π interactions as reflected from its lowest ³MMLCT emission energy and the complete switching-off of its monomeric emission, gives the most stable foldamer. Thus, it is believed that the two platinum(II) terpyridyl moieties at the termini have the ability to stabilize the short helical strands with five or six repeating units of mPE through the intramolecular Pt···Pt and π – π interactions in CH₃CN or at low temperature as depicted schematically in Figure 9.

In conclusion, we have designed a series of short meta-phenylene ethynylene foldamers as a first example which involves the use of metal···metal interaction to control the helix–coil folding transition. The versatile behavior of the Pt···Pt and π – π interactions of alkynylplatinum(II) terpyridyl moiety also provides an attractive spectroscopic probe for the study and understanding on the folding mechanism of metal-containing foldamers. It is envisaged

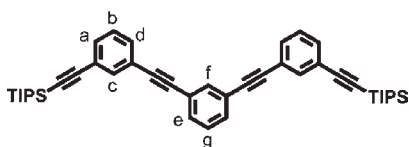
that metal···metal interactions will play an important role in the stabilization of helical strands in solution.

EXPERIMENTAL SECTION

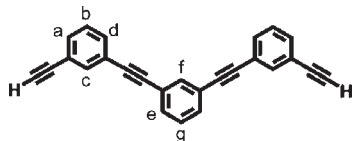
Materials and Reagents. Potassium tetrachloroplatinate(II) ($K_2[PtCl_4]$ (Chem. Pur., 98%)), 3-bromoiodobenzene (Apollo Scientific Ltd.), 1,3-diiodobenzene (Alfa Aesar Chemical Co. Ltd.), tetra-*n*-butylammonium fluoride (Sigma-Aldrich Co. Ltd., 1.0 M), trimethylsilylacetylene (GFS Chemical Co. Ltd.), triisopropylacetylene (GFS Chemical Co. Ltd.), and triethylamine (Apollo Scientific Ltd.) were purchased from the corresponding chemical company. Dichloromethane (Sigma-Aldrich Co. Ltd., ACS spectrophotometric grade) and acetonitrile (Acros Organics Co. Ltd., spectroscopic grade) were used for spectroscopic studies without further purification.

Synthesis. The synthetic schemes for ligands L1–L8 are given in the Supporting Information. All reactions were carried out under an inert atmosphere of nitrogen using standard Schlenk techniques.

Syntheses of L1–L8.

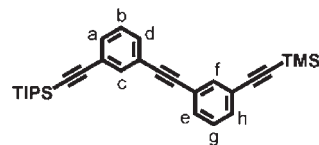


L1: To a 250-mL two-necked round-bottomed flask fitted with a magnetic stirrer were added 1,3-diiodobenzene (0.63 g, 1.9 mmol), bis(triphenylphosphine)palladium(II) dichloride (0.07 g, 0.1 mmol), tetrakis(triphenylphosphine)palladium(0) (0.11 g, 0.1 mmol), and copper(I) iodide (0.02 g, 0.1 mmol). The mixture was evacuated and flushed with nitrogen three times. Dry tetrahydrofuran (50 mL) and triethylamine (20 mL) were then transferred to the mixture. After stirring for 30 min, 1-ethynyl-3-triisopropylsilylethynylbenzene (1.24 g, 4.4 mmol) was then dropwise added by a syringe. The reaction mixture was heated to reflux for 48 h. The resulting mixture was evaporated to dryness and the residue was purified by column chromatography (70–230 mesh) using hexane as the eluent to give L1 as a colorless oil. Yield: 0.56 g (46%). 1H NMR (400 MHz, $CDCl_3$, 298 K, relative to Me_4Si): δ = 7.71 (t, 4J = 1.4 Hz, 1H, H_f), 7.67 (t, 4J = 1.4 Hz, 2H, H_c), 7.48 (m, 6H, H_a , H_d and H_e), 7.33 (t, 3J = 7.7 Hz, 1H, H_g), 7.31 (t, 3J = 7.7 Hz, 2H, H_b); 1.26 (m, 6H, $-Si\{CH(CH_3)_2\}_3$), 1.14 (d, 36H, $-Si\{CH(CH_3)_2\}_3$). ^{13}C NMR (100.6 MHz, $CDCl_3$, 298 K, relative to Me_4Si): 135.2, 134.6, 132.4, 131.4, 130.1, 128.4, 123.6, 123.5 (phenyl C), 89.7, 89.0, 82.4, 78.3 ($C\equiv C$), 18.7 (primary C on $-Si^iPr_3$ group), 11.3 (tertiary C on $-Si^iPr_3$ group). Positive FAB-MS: ion clusters at m/z 640.4 $[M]^+$. Elemental analyses calcd (%) for $C_{44}H_{54}Si_2$: C 82.69, H 8.52. Found: C 82.45, H 8.50.

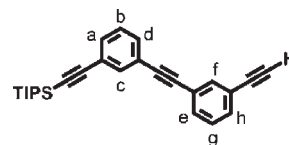


L2: To a solution of L1 (0.60 g, 0.9 mmol) and tetrahydrofuran (200 mL) was added a solution of tetra-*n*-butylammonium fluoride (0.1 M) in tetrahydrofuran (3 mL). The solution was stirred for 15 min and the solvent was removed. The brown solid was washed with plenty of methanol to give a white solid. Yield: 0.29 g (98%). 1H NMR (400 MHz, $CDCl_3$, 298 K, relative to Me_4Si): δ = 7.72 (t, 4J = 1.4 Hz, 1H, H_f), 7.69 (t, 4J = 1.4 Hz, 2H,

H_c), 7.50 (m, 6H, H_a , H_d and H_e), 7.34 (t, 3J = 7.7 Hz, 1H, H_g), 7.31 (t, 3J = 7.7 Hz, 2H, H_b); 3.12 (s, 2H, $-C\equiv CH$). ^{13}C NMR (100.6 MHz, $CDCl_3$, 298 K, relative to Me_4Si): 135.2, 134.7, 132.0, 131.9, 131.6, 128.5, 123.4, 122.6 (phenyl C), 89.1, 89.0, 82.7, 77.9 ($C\equiv C$). Positive FAB-MS: ion clusters at m/z 327.67 $[M]^+$. Elemental analyses calcd (%) for $C_{26}H_{14}$: C 95.68, H 4.32. Found: C 95.43, H 4.22.

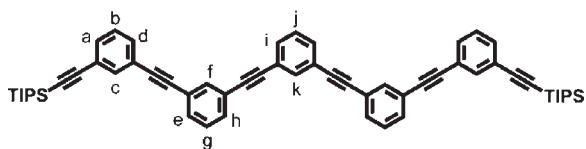


L3: To a 250-ml two-necked round-bottomed flask fitted with a magnetic stirrer were added 1-bromo-3-trimethylsilylethynylbenzene (6.15 g, 24.3 mmol), bis(triphenylphosphine)palladium(II) dichloride (0.85 g, 1.2 mmol), tetrakis(triphenylphosphine)palladium(0) (1.40 g, 1.2 mmol), and copper(I) iodide (0.23 g, 1.2 mmol). The mixture was evacuated and flushed with nitrogen three times. Dry tetrahydrofuran (500 mL) and dry triethylamine (150 mL) were then transferred to the mixture. 1-Ethynyl-3-triisopropylsilylethynylbenzene (6.86 g, 24.3 mmol) was then added dropwise by a syringe. The reaction was heated to reflux for 24 h. The resulting mixture was evaporated to dryness and the residue was purified by column chromatography (70–230 mesh) using hexane as the eluent to give L3 as a colorless oil. Yield: 7.62 g (69%). 1H NMR (400 MHz, $CDCl_3$, 298 K, relative to Me_4Si): δ = 7.63 (m, 2H, H_c and H_f), 7.44 (m, 4H, H_a , H_b , H_e and H_h), 7.28 (t, 3J = 7.8 Hz, 2H, H_b and H_f), 1.26 (m, 3H, $-Si\{CH(CH_3)_2\}_3$), 1.13 (d, 18H, $-Si\{CH(CH_3)_2\}_3$), 0.25 (s, 9H, $-Si(CH_3)_3$). ^{13}C NMR (100.6 MHz, $CDCl_3$, 298 K, relative to Me_4Si): 135.1, 131.9, 131.7, 131.3, 128.4, 123.9, 123.5, 123.3, 123.2 (phenyl C), 106.1, 104.1, 95.1, 91.5, 89.1, 89.0 ($C\equiv C$), 18.7 (primary C on $-Si^iPr_3$ group), 11.3 (tertiary C on $-Si^iPr_3$ group), 0.0 (primary C on $-SiMe_3$ group). Positive FAB-MS: ion clusters at m/z 555.0 $[M]^+$. Elemental analyses calcd (%) for $C_{38}H_{42}Si_2$: C 82.25, H 7.63. Found: C 82.07, H 7.70.

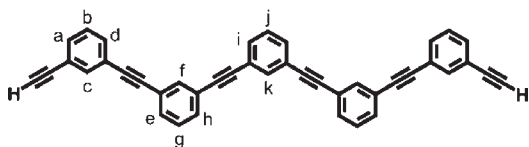


L4: To a solution of L3 (8.74 g, 19.3 mmol) in tetrahydrofuran (200 mL) and methanol (50 mL) was added potassium carbonate (7.97 g, 57.8 mmol). The solution was stirred overnight. The reaction mixture was diluted with dichloromethane (500 mL) and brine (250 mL). The organic phase was washed with brine three times, and dried over anhydrous $MgSO_4$. The solvent was removed, and the resulting oil was purified by column chromatography (70–230 mesh) using hexane as the eluent to give L4 as a colorless oil. Yield: 6.62 g (90%). 1H NMR (400 MHz, $CDCl_3$, 298 K, relative to Me_4Si): δ = 7.66 (t, 3J = 1.1 Hz, 1H, H_f), 7.64 (t, 3J = 1.1 Hz, 1H, H_c), 7.49 (dt, 3J = 7.7 Hz, 4J = 1.3 Hz, 1H, H_e), 7.44 (m, 3H, H_a , H_d and H_h), 7.31 (t, 3J = 7.8 Hz, 1H, H_g), 7.29 (t, 3J = 7.8 Hz, 1H, H_b), 3.16 (s, 1H, $-C\equiv CH$), 1.26 (m, 3H, $-Si\{CH(CH_3)_2\}_3$), 1.13 (d, 18H, $-Si\{CH(CH_3)_2\}_3$). ^{13}C NMR (100.6 MHz, $CDCl_3$, 298 K, relative to Me_4Si): 135.2, 135.1, 132.1, 132.0, 131.9, 131.3, 128.5, 128.4, 124.0, 123.4, 123.1, 122.5 (phenyl C), 91.5, 89.2, 88.8, 82.7 ($C\equiv C$), 18.7 (primary C on $-Si^iPr_3$ group), 11.3 (tertiary C on $-Si^iPr_3$ group). Positive FAB-MS: ion clusters at m/z 383.61

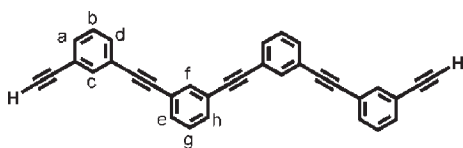
[M]⁺. Elemental analyses calcd (%) for C₂₇H₃₀Si: C 87.08, H 7.10. Found: C 87.29, H 7.21.



L5: The titled compound was prepared according to the procedure similar to that described for the preparation of **L1**, except **L4** (1.68 g, 4.4 mmol) was used in place of 1-ethynyl-3-triisopropylsilylethynylbenzene to give **L5** as a colorless oil. Yield: 0.72 g (45%). ¹H NMR (400 MHz, CDCl₃, 298 K, relative to Me₄Si): δ = 7.72 (t, ⁴J = 1.5 Hz, 2H, H_f), 7.66 (t, ⁴J = 1.5 Hz, 1H, H_k), 7.50 (m, 6H, H_e, H_h and H_i), 7.47 (dt, ³J = 7.7 Hz, ⁴J = 1.3 Hz, 2H, H_d), 7.45 (dt, ³J = 7.9 Hz, ⁴J = 1.3 Hz, 2H, H_a), 7.36 (t, ³J = 7.7 Hz, 1H, H_j), 7.35 (t, ³J = 7.7 Hz, 2H, H_g), 7.30 (t, ³J = 7.8 Hz, 2H, H_b), 1.26 (m, 6H, –Si{CH(CH₃)₂}₃), 1.14 (d, 36H, –Si{CH(CH₃)₂}₃). ¹³C NMR (100.6 MHz, CDCl₃, 298 K, relative to Me₄Si): 135.3, 134.6, 133.7, 131.8, 131.5, 123.7, 123.6, 122.3 (phenyl C), 89.8, 89.5, 88.5, 83.4, 79.3 (C≡C), 18.7 (primary C on –SiⁱPr₃ group), 11.3 (tertiary C on –SiⁱPr₃ group). Positive FAB-MS: ion clusters at *m/z* 840.3 [M]⁺. Elemental analyses calcd (%) for C₆₀H₆₂Si₂: C 87.08, H 7.10. Found: C 87.00, H 7.31.

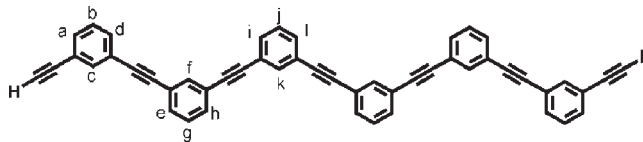


L6: The titled compound was prepared according to the procedure similar to that described for the preparation of **L2**, except **L5** (0.76 g, 0.9 mmol) was used in place of **L1** to give a white solid. Yield: 0.43 g (90%). ¹H NMR (400 MHz, CDCl₃, 298 K, relative to Me₄Si): δ = 7.71 (t, ⁴J = 1.4 Hz, 1H, H_k), 7.69 (t, ⁴J = 1.4 Hz, 2H, H_f), 7.67 (t, ⁴J = 1.4 Hz, 2H, H_c), 7.51 (m, 6H, H_e, H_h and H_i), 7.47 (dt, ³J = 7.7 Hz, ⁴J = 1.3 Hz, 2H, H_d), 7.45 (dt, ³J = 7.7 Hz, ⁴J = 1.3 Hz, 2H, H_a), 7.37 (t, ³J = 7.7 Hz, 1H, H_j), 7.35 (t, ³J = 7.7 Hz, 2H, H_g), 7.33 (t, ³J = 7.6 Hz, 2H, H_b), 3.09 (s, 2H, –C≡CH). ¹³C NMR (100.6 MHz, CDCl₃, 298 K, relative to Me₄Si): 135.2, 134.7, 132.0, 131.6, 131.5, 128.6, 128.5, 123.4, 122.6 (phenyl C), 89.2, 89.1, 89.0, 82.7, 79.2, 79.0, 77.9 (C≡C). Positive FAB-MS: ion clusters at *m/z* 527.8 [M]⁺. Elemental analyses calcd (%) for C₄₂H₂₂: C 95.79, H 4.21. Found: C 95.85, H 4.17.



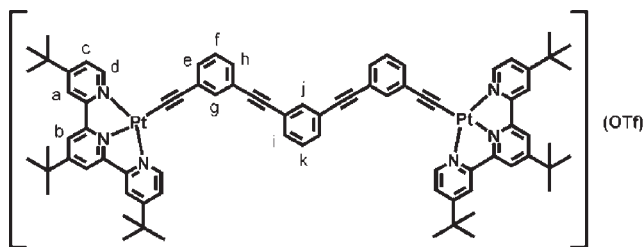
L7: The titled compound was prepared according to the procedure similar to that described for the preparation of **L3**, except 3,3'-bis(ethynyl)tolane (2.7 g, 12.1 mmol) was used in place of 1-ethynyl-3-triisopropylsilylethynylbenzene and then followed by the deprotection of TMS with TBAF to give **L7** as a white

solid. Yield: 4.12 g (80%). ¹H NMR (400 MHz, CDCl₃, 298 K, relative to Me₄Si): δ = 7.70 (t, ⁴J = 1.4 Hz, 2H, H_f), 7.69 (t, ⁴J = 1.4 Hz, 2H, H_c), 7.48 (m, 8H, H_e, H_d, H_g and H_h), 7.36 (t, ³J = 7.7 Hz, 2H, H_g), 7.32 (t, ³J = 7.7 Hz, 2H, H_b), 3.09 (s, 2H, –C≡CH). ¹³C NMR (100.6 MHz, CDCl₃, 298 K, relative to Me₄Si): 138.6, 137.5, 132.0, 130.4, 125.7, 124.4 (phenyl C), 89.5, 89.3, 84.2, 80.0, 77.4 (C≡C). Positive FAB-MS: ion clusters at *m/z* 427.5 [M]⁺. Elemental analyses calcd (%) for C₃₄H₁₈: C 95.75, H 4.25. Found: C 95.64, H 4.20.



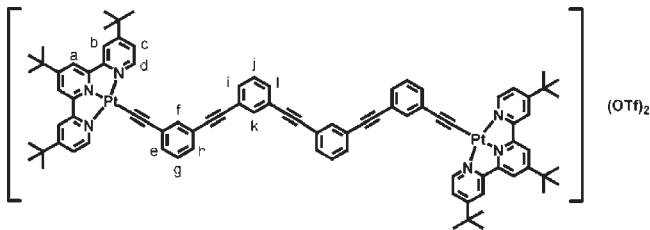
L8: The titled compound was prepared according to the procedure similar to that described for the preparation of **L3**, except **L7** (5.15 g, 12.1 mmol) was used in place of 1-ethynyl-3-triisopropylsilylethynylbenzene and then followed by the deprotection of TMS with TBAF to give **L8** as a white solid. Yield: 5.45 g (72%). ¹H NMR (400 MHz, CDCl₃, 298 K, relative to Me₄Si): δ = 7.73 (t, ⁴J = 1.4 Hz, 2H, H_k), 7.71 (t, ⁴J = 1.4 Hz, 2H, H_f), 7.66 (t, ⁴J = 1.4 Hz, 2H, H_c), 7.49 (m, 10H, H_e, H_d, H_g, H_h, H_i and H_l), 7.43 (dt, ³J = 7.7 Hz, ⁴J = 1.3 Hz, 2H, H_a), 7.36 (t, ³J = 7.7 Hz, 2H, H_j), 7.35 (t, ³J = 7.7 Hz, 2H, H_g), 7.29 (t, ³J = 7.6 Hz, 2 H, H_b), 3.10 (s, 2H, –C≡CH). ¹³C NMR (100.6 MHz, CDCl₃, 298 K, relative to Me₄Si): 135.2, 134.7, 132.0, 131.6, 131.5, 128.6, 128.5, 123.5, 123.4, 122.6 (phenyl C), 89.2, 89.1, 89.0, 82.7, 79.2, 79.0, 77.9 (C≡C). Positive FAB-MS: ion clusters at *m/z* 627.7 [M]⁺. Elemental analyses calcd (%) for C₅₀H₂₆: C 95.82, H 4.18. Found: C 95.98, H 4.24.

Syntheses of 1–6.

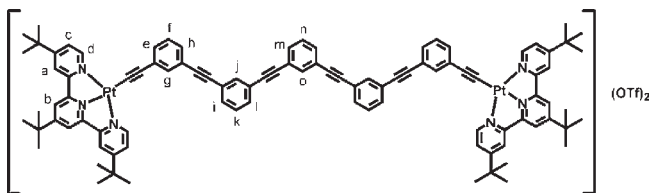


1: To a solution of **L2** (30 mg, 0.09 mmol) and [(^tBu₃tpy)PtCl] (OTf)₂ (143 mg, 0.18 mmol) in degassed *N,N*-dimethylformamide (30 mL) containing triethylamine (5 mL) was added a catalytic amount of CuI. The solution was stirred overnight at room temperature. After removing the solvent, the reaction mixture was purified by chromatography on silica gel using dichloromethane–acetone mixture (10:1 v/v) as eluent, followed by the diffusion of diethyl ether vapor into acetonitrile solution to give **1** as a yellow solid. Yield: 100 mg (60%). ¹H NMR (500 MHz, CD₃CN, 298 K, relative to Me₄Si): δ = 8.89 (d with Pt satellites, ³J = 6.0 Hz, 4H, H_d), 8.21 (s, 4H, H_b), 8.15 (d, ⁴J = 1.9 Hz, 4H, H_a), 7.66 (t, ⁴J = 1.3 Hz, 1H, H_j), 7.62 (t, ⁴J = 1.3 Hz, 2H, H_g), 7.60 (dd, ³J = 6.0 Hz, ⁴J = 2.1 Hz, 4H, H_c), 7.47 (dd, ³J = 8.2 Hz, ⁴J = 1.3 Hz, 2H, H_i), 7.42 (dt, ³J = 7.7 Hz, ⁴J = 1.3 Hz, 2H, H_e), 7.36 (dt, ³J = 7.7 Hz, ⁴J = 1.3 Hz, 2H, H_h), 7.31 (t, ³J = 7.7 Hz, 3H, H_f and H_l), 1.59 (s, 18H, –^tBu), 1.51 (s, 36H, –^tBu). ¹³C NMR (125.8 MHz, CD₃CN, 298 K, relative to Me₄Si): δ = 168.5, 167.8, 159.6, 155.0 (quaternary C on terpyridyl), 154.8 (tertiary C on terpyridyl), 135.7, 135.2, 133.2, 132.5,

130.4, 130.3, 129.8, 128.5, 124.4, 124.1 (phenyl C), 126.8, 123.7, 122.2 (tertiary C on terpyridyl), 103.6 (Pt–C≡C), 101.2 (Pt–C≡C), 90.8, 89.5, (C≡C), 38.1, 37.1 (quaternary C on ^tBu), 30.7, 30.3 (primary C on ^tBu). IR (nujol): $\nu = 2119 \text{ cm}^{-1}$ (C≡C). Positive FAB-MS: ion clusters at m/z 760.7 [$M - 2\text{OTf}$]²⁺. Elemental analyses calcd (%) for C₈₂H₈₂F₆N₆O₆Pt₂S₂: C 54.24, H 4.55, N 4.63. Found: C 54.41, H 4.56, N 4.67.

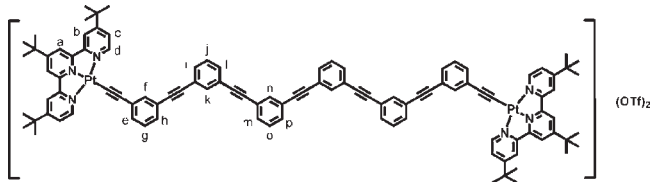


2: The titled complex was prepared according to the procedure similar to that described for the preparation of 1, except L7 (39 mg, 0.09 mmol) was used in place of L2. Yield: 116 mg (67%). ¹H NMR (500 MHz, CD₃CN, 330 K, relative to Me₄Si): $\delta = 8.78$ (d with Pt satellites, ³J = 6.0 Hz, 4H, H_d), 8.17 (s, 4H, H_a), 8.12 (d, ⁴J = 2.0 Hz, 4H, H_b), 7.82 (t, ⁴J = 1.3 Hz, 2H, H_f), 7.62 (t, ⁴J = 1.3 Hz, 2H, H_k), 7.64 (dd, ³J = 6.0 Hz, ⁴J = 2.1 Hz, 4H, H_c), 7.60 (m, 4H, H_e and H_h), 7.57 (dt, ³J = 7.1 Hz, ⁴J = 1.7 Hz, 2H, H_i), 7.48 (m, 4H, H_g and H_l), 7.44 (t, ³J = 7.8 Hz, 2H, H_j), 1.51 (s, 18H, ^tBu), 1.46 (s, 36H, ^tBu). ¹³C NMR (125.8 MHz, CD₃CN, 298 K, relative to Me₄Si): $\delta = 168.5, 168.0, 159.8, 155.1$ (quaternary C on terpyridyl), 154.4 (tertiary C on terpyridyl), 137.6, 137.4, 134.5, 130.4, 130.1, 130.9, 125.4, 124.4, 124.3, 124.2, 123.6 (phenyl C), 127.0, 123.4, 122.6 (tertiary C on terpyridyl), 103.1 (Pt–C≡C), 101.0 (Pt–C≡C), 91.8, 90.1, 89.6, 89.5 (C≡C), 38.2, 37.1 (quaternary C on ^tBu), 30.8, 30.4 (primary C on ^tBu). IR (nujol): 2120 cm^{-1} (C≡C). Positive FAB-MS: ion clusters at m/z 809.3 [$M - 2\text{OTf}$]²⁺. Elemental analyses calcd (%) for C₉₀H₈₆F₆N₆O₆Pt₂S₂: C 56.42, H 4.52, N 4.39. Found: C 56.14, H 4.44, N 4.45.

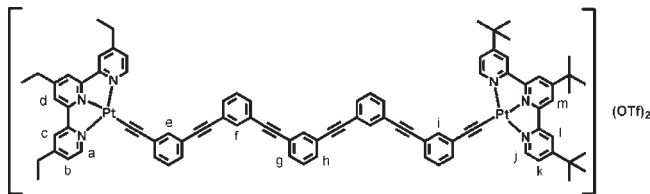


3: The titled complex was prepared according to the procedure similar to that described for the preparation of 1, except L6 (47 mg, 0.09 mmol) was used in place of L2. Yield: 96 mg (53%). ¹H NMR (500 MHz, CD₃CN, 298 K, relative to Me₄Si): $\delta = 8.71$ (d with Pt satellites, ³J = 6.0 Hz, 4H, H_d), 8.18 (s, 4H, H_b), 8.03 (d, ⁴J = 2.0 Hz, 4H, H_a), 7.83 (t, ⁴J = 1.3 Hz, 2H, H_g), 7.78 (t, ⁴J = 1.3 Hz, 1H, H_o), 7.71 (dd, ³J = 6.0 Hz, ⁴J = 2.1 Hz, 4H, H_c), 7.64 (m, 4H, H_e and H_m), 7.57 (m, 4H, H_h and H_i), 7.51 (t, ³J = 7.8 Hz, 1H, H_n), 7.50 (t, ³J = 7.8 Hz, 2H, H_p), 7.43 (dt, ³J = 7.1 Hz, ⁴J = 1.7 Hz, 2H, H_i), 7.39 (t, ³J = 7.4 Hz, 2H, H_e), 7.37 (dt, ³J = 7.1 Hz, ⁴J = 1.7 Hz, 2H, H_i), 1.58 (s, 18H, ^tBu), 1.48 (s, 36H, ^tBu). ¹³C NMR (125.8 MHz, CD₃CN, 298 K, relative to Me₄Si): $\delta = 168.5, 167.9, 159.8, 155.1$ (quaternary C on terpyridyl), 154.4 (tertiary C on terpyridyl), 136.5, 135.5, 135.1, 134.7, 132.8, 132.7, 132.6, 132.4, 130.4, 130.1, 129.9, 128.4, 124.4, 124.3, 124.2, 123.8 (phenyl C), 126.9, 123.8, 122.2 (tertiary C on terpyridyl), 103.2 (Pt–C≡C), 101.0 (Pt–C≡C), 90.8, 90.0, 89.8, 89.4 (C≡C), 38.2, 37.1 (quaternary C on ^tBu), 30.8, 30.4

(primary C on ^tBu). IR (nujol): 2122 cm^{-1} (C≡C). Positive FAB-MS: ion clusters at m/z 858.3 [$M - 2\text{OTf}$]²⁺. Elemental analyses calcd (%) for C₉₈H₉₀F₆N₆O₆Pt₂S₂·CHCl₃: C 55.68, H 4.30, N 3.94. Found: C 55.73, H 4.47, N 3.86.

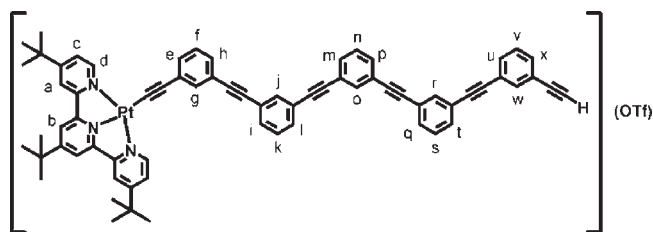


4: The titled complex was prepared according to the procedure similar to that described for the preparation of 1, except L8 (57 mg, 0.09 mmol) was used in place of L2. Yield: 106 mg (56%). ¹H NMR (500 MHz, CD₃CN, 330 K, relative to Me₄Si): $\delta = 8.84$ (d with Pt satellites, ³J = 6.0 Hz, 4H, H_d), 8.18 (s, 4H, H_a), 8.13 (d, ⁴J = 2.0 Hz, 4H, H_b), 7.72 (t, ⁴J = 1.3 Hz, 2H, H_f), 7.71 (t, ⁴J = 1.3 Hz, 2H, H_k), 7.64 (dd, ³J = 6.0 Hz, ⁴J = 2.1 Hz, 4H, H_c), 7.61 (dt, ³J = 7.1 Hz, ⁴J = 1.7 Hz, 2H, H_i), 7.59 (dt, ³J = 7.1 Hz, ⁴J = 1.7 Hz, 2H, H_i), 7.48 (m, 8H, H_g, H_l and H_h), 7.44 (t, ³J = 7.8 Hz, 2H, H_j), 7.26 (dt, ³J = 7.1 Hz, ⁴J = 1.7 Hz, 2H, H_m), 7.22 (dt, ³J = 7.1 Hz, ⁴J = 1.7 Hz, 2H, H_p), 7.19 (dt, ³J = 7.1 Hz, ⁴J = 1.7 Hz, 2H, H_o), 1.51 (s, 18H, ^tBu), 1.46 (s, 36H, ^tBu). ¹³C NMR (125.8 MHz, CD₃CN, 298 K, relative to Me₄Si): $\delta = 168.5, 168.0, 159.8, 155.1$ (quaternary C on terpyridyl), 154.4 (tertiary C on terpyridyl), 137.5, 137.4, 134.8, 136.4, 136.2, 132.4, 130.4, 130.1, 130.9, 125.4, 124.4, 124.3, 124.2, 123.6 (phenyl C), 126.9, 123.8, 122.2 (tertiary C on terpyridyl), 103.3 (Pt–C≡C), 101.1 (Pt–C≡C), 91.8, 90.1, 89.6, 89.5 (C≡C), 38.2, 37.1 (quaternary C on ^tBu), 30.8, 30.4 (primary C on ^tBu). IR (nujol): 2120 cm^{-1} (C≡C). Positive FAB-MS: ion clusters at m/z 910.1 [$M - 2\text{OTf}$]²⁺. Elemental analyses calcd (%) for C₁₀₆H₉₄F₆N₆O₆Pt₂S₂·2CHCl₃: C 55.08, H 4.11, N 3.57. Found: C 55.18, H 4.40, N 3.45.



5: To a solution of 6 (24 mg, 0.02 mmol) and [(Et₃trpy)PtCl]-(OTf) (13 mg, 0.02 mmol) in degassed N,N-dimethylformamide (30 mL) containing triethylamine (5 mL) was added a catalytic amount of CuI. The solution was stirred overnight at room temperature. After removing the solvent, the reaction mixture was purified by chromatography on silica gel using dichloromethane-acetone mixture (10:1 v/v) as eluent, followed by the diffusion of diethyl ether vapor into acetonitrile solution to give 5 as an orange solid. Yield: 20 mg (56%). ¹H NMR (500 MHz, CD₃CN, 350 K, relative to Me₄Si): $\delta = 8.72$ (d with Pt satellites, ³J = 6.0 Hz, 2H, H_a), 8.67 (d with Pt satellites, ³J = 6.0 Hz, 2H, H_i), 8.19 (s, 2H, H_d), 8.03 (d, ⁴J = 2.0 Hz, 2H, H_c), 7.95 (s, 2H, H_m), 7.90 (t, ⁴J = 1.3 Hz, 1H, H_e), 7.86 (t, ⁴J = 1.3 Hz, 1H, H_i), 7.85 (t, ⁴J = 1.3 Hz, 1H, H_p), 7.81 (d, ⁴J = 2.0 Hz, 2H, H_l), 7.75 (dd, ³J = 6.0 Hz, ⁴J = 2.1 Hz, 2H, H_b), 7.65 (m, 5H, phenyl H_s), 7.60 (dt, ³J = 7.1 Hz, ⁴J = 1.7 Hz, 1H, phenyl H), 7.56 (dd, ³J = 6.0 Hz, ⁴J = 2.1 Hz, 2H, H_k), 7.50 (m, 6H, phenyl H_s), 7.44 (m, 5H, phenyl H_s), 7.36 (dt, ³J = 7.1 Hz, ⁴J = 1.7 Hz, 1H, H_g), 7.33 (dt, ³J = 7.1 Hz, ⁴J = 1.7 Hz, 1H, H_h), 2.97 (q, 2H, –CH₂–), 2.93 (q, 4H, –CH₂–),

1.57 (s, 9H, $-t$ Bu), 1.44 (t, 3H, $-CH_3$), 1.40 (s, 18H, $-t$ Bu), 1.32 (t, 6H, $-CH_3$). ^{13}C NMR (125.8 MHz, CD_3CN , 298 K, relative to Me_4Si): δ = 168.5, 168.0, 161.3, 160.9, 160.0, 159.7, 155.2, 155.0 (quaternary C on terpyridyl), 154.1, 153.9 (tertiary C on terpyridyl), 137.0, 136.6, 135.7, 135.3, 134.9, 133.0, 132.7, 132.6, 132.5, 132.4, 132.2, 130.5, 130.4, 130.2, 130.1, 130.0, 129.9, 129.0, 127.0, 126.0, 124.5, 124.3, 124.2, 124.1, 123.6 (phenyl C), 128.4, 128.3, 124.0, 123.9, 122.2, 120.3 (tertiary C on terpyridyl), 102.9, 102.6 (Pt–C \equiv C), 101.0, 100.3 (Pt–C \equiv C), 96.3, 91.3, 90.9, 90.8, 90.0, 89.9, 89.8, 89.7 (C \equiv C), 38.2, 37.1 (quaternary C on $-t$ Bu), 38.0, 37.5 (secondary C on $-Et$), 30.9, 30.3 (primary C on $-Et$), 30.8, 30.4 (primary C on $-t$ Bu). IR (nujol): 2120 cm^{-1} (C \equiv C). Positive FAB-MS: ion clusters at m/z 818.8 [$M - 2OTf$] $^{2+}$. Elemental analyses calcd (%) for $C_{92}H_{78}F_6N_6O_6Pt_2S_2$: C 57.66, H 4.20, N 4.80. Found: C 57.80, H 4.10, N 4.59.



6: To a solution of **L6** (168 mg, 0.32 mmol) and [$(t$ Bu $_3$ trpy)PtCl] $-(OTf)_2$ (250 mg, 0.32 mmol) in degassed *N,N*-dimethylformamide (30 mL) containing triethylamine (5 mL) was added a catalytic amount of CuI. The solution was stirred overnight at room temperature. After removing the solvent, the reaction mixture was purified by chromatography on silica gel using dichloromethane–acetone mixture (10:1 v/v) as eluent, followed by the diffusion of diethyl ether vapor into acetonitrile solution to give **6** as a yellow solid. Yield: 110 mg (27%). 1H NMR (500 MHz, CD_3CN , 298 K, relative to Me_4Si): δ = 8.91 (d with Pt satellites, $^3J = 6.0$ Hz, 2H, H_d), 8.21 (s, 2H, H_b), 8.13 (d, $^4J = 1.9$ Hz, 2H, H_a), 7.66 (m, 2H, H_g and H_j), 7.65 (t, $^4J = 1.2$ Hz, 1H, H_o), 7.63 (t, $^4J = 1.2$ Hz, 1H, H_r), 7.59 (dd, $^3J = 6.0$ Hz, $^4J = 2.1$ Hz, 2H, H_c), 7.57 (t, $^4J = 1.4$ Hz, 1H, H_w), 7.47 (m, 8H, H_e , H_f , H_h , H_i , H_k , H_l , H_m , and H_p), 7.41 (dt, $^3J = 7.8$ Hz, $^4J = 1.4$ Hz, 1H, H_u), 7.36 (m, 4H, H_n , H_q , H_t and H_x), 7.32 (t, $^3J = 7.5$ Hz, 1H, H_s), 7.31 (t, $^3J = 7.5$ Hz, 1H, H_v), 3.41 (s, 1H, $-C\equiv CH$), 1.58 (s, 9H, $-t$ Bu), 1.48 (s, 18H, $-t$ Bu). ^{13}C NMR (125.8 MHz, CD_3CN , 298 K, relative to Me_4Si): δ = 168.4, 167.7, 159.6, 154.9 (quaternary C on terpyridyl), 154.8 (tertiary C on terpyridyl), 135.8, 135.6, 135.4, 135.3, 135.2, 133.1, 132.9, 132.7, 132.6, 132.5, 132.4, 132.3, 130.3, 130.2, 130.1, 130.0, 129.8, 128.6, 124.4, 124.2, 124.1, 124.0, 123.7 (phenyl C), 126.7, 123.5, 122.2 (tertiary C on terpyridyl), 103.5 (Pt–C \equiv C), 101.1 (Pt–C \equiv C), 90.9, 90.0, 89.9, 89.8, 89.5, 83.2, 79.9 (C \equiv C), 38.1, 37.1 (quaternary C on $-t$ Bu), 30.7, 30.3 (primary C on $-t$ Bu). IR (nujol): ν = 2118 cm^{-1} (C \equiv C). Positive FAB-MS: ion clusters at m/z 1123 [$M - OTf$] $^+$. Elemental analyses calcd (%) for $C_{70}H_{56}F_3N_3O_3Pt \cdot 3CHCl_3$: C 56.25, H 3.67, N 2.43. Found: C 56.83, H 3.45, N 2.67.

Physical Measurements and Instrumentation. 1H NMR spectra were recorded on a Bruker AVANCE 400 and 500 (400 and 500 MHz) Fourier-transform NMR spectrometer with chemical shifts reported relative to tetramethylsilane, $(CH_3)_4Si$. Negative-ion FAB mass spectra were recorded on a Thermo Scientific DFS high resolution magnetic sector mass spectrometer. IR spectra were obtained as KBr disk on a Bio-Rad FTS-7 Fourier transform infrared spectrophotometer (4000–400 cm^{-1}). Elemental analyses of complexes were performed on a Flash EA 1112 elemental analyzer at the Institute of Chemistry,

Chinese Academy of Sciences. The UV–visible spectra were obtained using a Hewlett-Packard 8452A diode array spectrophotometer. Emission spectra at room temperature were recorded on a Spex Fluorolog-3 model FL3-211 fluorescence spectrofluorometer equipped with an R2658P PMT detector. Variable-temperature UV–vis absorption and emission spectra were obtained using a Varian Cary 50 UV–vis spectrophotometer and a Spex Fluorolog-3 model FL3-211 fluorescence spectrofluorometer equipped with an R2658P PMT detector, respectively. The temperature was maintained by a Varian Cary Single cell Peltier thermostat.

■ ASSOCIATED CONTENT

S Supporting Information. The synthetic routes for *meta*-phenylene ethynylene oligomers ($n = 3, 4, 5, 6$). Variable-temperature 1H NMR experiments for **3–5** in $CDCl_3$ and CD_3CN . Calculation of the distances between protons on *m*PE and 4'- and 4''- t Bu groups for **3** in CH_3CN . UV–vis absorption spectra of **1, 2**, and **6** in CH_2Cl_2 and CH_3CN at 298 K. UV–vis absorption spectral traces of **4** in CH_2Cl_2 with increasing CH_3CN content at 298 K and decreasing the temperature from 353 to 293 K. Calculation of helix stabilization energy of **3–5**. Emission spectral traces for **4** in $CH_3CN-CH_2Cl_2$ upon increasing the CH_3CN fraction and decreasing the temperature from 353 to 293 K. Emission spectra of **1, 2**, and **6** in CH_2Cl_2 and CH_3CN at 298 K. This material is available free of charge via the Internet at <http://pubs.acs.org>.

■ AUTHOR INFORMATION

Corresponding Author
wyyam@hku.hk

■ ACKNOWLEDGMENT

V.W.-W.Y. acknowledges the support from The University of Hong Kong under the Distinguished Research Achievement Award Scheme and the URC Strategic Research Theme on Molecular Materials. This work has been supported by the University Grants Committee Areas of Excellence (AoE) Scheme (AoE/P-03/08) and a General Research Fund (GRF) grant from the Research Grants Council of Hong Kong Special Administrative Region, P. R. China (HKU 7060/09P). S.Y.-L.L. acknowledges the receipt of a postgraduate studentship and A.Y.-Y.T. acknowledges the receipt of a University Postdoctoral Fellowship, both administered by The University of Hong Kong.

■ REFERENCES

- (1) (a) Connick, W. B.; Marsh, R. E.; Schaefer, W. P.; Gray, H. B. *Inorg. Chem.* **1997**, *36*, 913–922. (b) Herber, R. H.; Croft, M.; Coyer, M. J.; Bilash, B.; Sahiner, A. *Inorg. Chem.* **1994**, *33*, 2422–2426. (c) Miskowski, V. M.; Houlding, V. H. *Inorg. Chem.* **1991**, *30*, 4446–4452. (d) Miskowski, V. M.; Houlding, V. H. *Inorg. Chem.* **1989**, *28*, 1529–1533. (e) Kunkely, H.; Vogler, A. *J. Am. Chem. Soc.* **1990**, *112*, 5625–5625.
- (2) (a) Arena, G.; Calogero, G.; Campagna, S.; Scolaro, L. M.; Ricevuto, V.; Romeo, R. *Inorg. Chem.* **1998**, *37*, 2763–2769. (b) Yip, H. K.; Cheng, L. K.; Cheung, K. K.; Che, C. M. *J. Chem. Soc., Dalton Trans.* **1993**, *19*, 2933–2938. (c) Büchner, R.; Cunningham, C. T.; Field, J. S.; Haines, R. J.; McMillin, D. R.; Summerton, G. C. *J. Chem. Soc., Dalton Trans.* **1999**, *5*, 711–718. (d) Bailey, J. A.; Hill, M. G.; Marsh, R. E.; Miskowski, V. M.; Schaefer, W. P.; Gray, H. B. *Inorg. Chem.* **1995**, *34*, 4591–4599. (e) Wong, K. M. C.; Zhu, N.; Yam, V. W. W. *Chem. Commun.* **2006**, *32*, 3441–3443. (f) Jennette, K. W.; Gill, J. T.;

Sadowick, J. A.; Lippard, S. J. *J. Am. Chem. Soc.* **1976**, *98*, 6159–6168. (g) Aldrige, T. K.; Stacy, E. M.; McMillin, D. R. *Inorg. Chem.* **1994**, *33*, 722–727. (h) Hill, M. G.; Bailey, J. A.; Miskowski, V. M.; Gray, H. B. *Inorg. Chem.* **1996**, *35*, 4585–4590.

(3) (a) Yam, V. W. W.; Wong, K. M. C.; Zhu, N. *J. Am. Chem. Soc.* **2002**, *124*, 6506–6507. (b) Yam, V. W. W.; Tang, R. P. L.; Wong, K. M. C.; Cheung, K. K. *Organometallics* **2001**, *20*, 4476–4482. (c) Yam, V. W. W.; Chan, K. H. Y.; Wong, K. M. C.; Zhu, N. *Chem.—Eur. J.* **2005**, *11*, 4535–4543. (d) Yu, C.; Wong, K. M. C.; Chan, K. H. Y.; Yam, V. W. W. *Angew. Chem., Int. Ed.* **2005**, *44*, 791–794. (e) Yu, C.; Chan, K. H. Y.; Wong, K. M. C.; Yam, V. W. W. *Chem.—Eur. J.* **2008**, *14*, 4577–4584. (f) Chan, K. H. Y.; Lam, W. Y.; Wong, K. M. C.; Tang, B. Z.; Yam, V. W. W. *Chem.—Eur. J.* **2009**, *15*, 2328–2334. (g) Tam, A. Y. Y.; Wong, K. M. C.; Wang, G.; Yam, V. W. W. *Chem. Commun.* **2007**, *20*, 2028–2030. (h) Tam, A. Y. Y.; Wong, K. M. C.; Yam, V. W. W. *Chem.—Eur. J.* **2009**, *19*, 4775–4778. (i) Tam, A. Y. Y.; Wong, K. M. C.; Zhu, N.; Yam, V. W. W. *Langmuir* **2009**, *15*, 8685–8695. (j) Yu, C.; Chan, K. H. Y.; Wong, K. M. C.; Yam, V. W. W. *Proc. Natl. Acad. Sci. U.S.A.* **2006**, *103*, 19652–19657. (k) Yu, C.; Chan, K. H. Y.; Wong, K. M. C.; Yam, V. W. W. *Chem. Commun.* **2009**, *25*, 3756–3758. (l) Yeung, M. C. L.; Wong, K. M. C.; Tsang, Y. K. T.; Yam, V. W. W. *Chem. Commun.* **2010**, *46*, 7709–7711. (m) Yam, V. W. W.; Chan, K. H. Y.; Wong, K. M. C.; Chu, B. W. K. *Angew. Chem., Int. Ed.* **2006**, *45*, 6169–6173. (n) Chan, K. H. Y.; Chow, H. S.; Wong, K. M. C.; Yeung, M. C. L.; Yam, V. W. W. *Chem. Sci.* **2010**, *1*, 477–482. (o) Wong, K. M. C.; Yam, V. W. W. *Acc. Chem. Res.* **2011**, *44*, 424–434. (p) Lo, H. S.; Yip, S. K.; Zhu, N.; Yam, V. W. W. *Dalton Trans.* **2007**, *39*, 4386–4389.

(4) (a) Yam, V. W. W.; Wong, K. M. C.; Zhu, N. *Angew. Chem., Int. Ed.* **2003**, *42*, 1400–1403. (b) Wong, K. M. C.; Tang, W. S.; Lu, X. X.; Zhu, N.; Yam, V. W. W. *Inorg. Chem.* **2005**, *44*, 1492–1498. (c) Zhu, M. X.; Lu, W.; Zhu, N.; Che, C. M. *Chem.—Eur. J.* **2008**, *14*, 9736–9746. (d) Kui, S. C. F.; Law, Y. C.; Tong, G. S. M.; Lu, W.; Yuen, M. Y.; Che, C. M. *Chem. Sci.* **2011**, *2*, 221–228.

(5) (a) Hill, D. J.; Mio, M. J.; Prince, R. B.; Hughes, T. S.; Moore, J. S. *Chem. Rev.* **2001**, *101*, 3893–4012. (b) Nelson, J. C.; Saven, J. G.; Moore, J. S.; Wolynes, P. G. *Science* **1997**, *277*, 1793–1796. (c) *Foldamers: Structure, Properties and Applications*; Hecht, S.; Huc, I., Eds.; Wiley-VCH: Weinheim, 2007; (d) Ferrand, Y.; Gan, Q.; Kauffmann, B.; Jiang, H.; Huc, I. *Angew. Chem., Int. Ed.* **2011**, *33*, 7572–7575. (e) Guichard, G.; Huc, I. *Chem. Commun.* **2011**, *21*, 5933–5941. (f) Gan, Q.; Ferrand, Y.; Bao, C.; Kauffmann, B.; Grelard, A.; Jiang, H.; Huc, I. *Science* **2011**, *1172*–1175.

(6) (a) Berl, V.; Huc, I.; Khoury, R. G.; Krische, M. J.; Lehn, J. M. *Nature* **2000**, *407*, 720–723. (b) Kolomiets, E.; Berl, V.; Odriozola, I.; Stadler, A. M.; Kyritsakas, N.; Lehn, J. M. *Chem. Commun.* **2003**, *23*, 2868–2869. (c) Haldar, D.; Jiang, H.; Leger, J. M.; Huc, I. *Angew. Chem., Int. Ed.* **2006**, *45*, 5483–5486. (d) Bao, C.; Kauffmann, B.; Gan, Q.; Srinivas, K.; Jiang, H.; Huc, I. *Angew. Chem., Int. Ed.* **2008**, *120*, 4153–4156. (e) Gillies, E. R.; Deiss, F.; Staedel, C.; Schmitter, J. M.; Huc, I. *Angew. Chem., Int. Ed.* **2007**, *46*, 4081–4084. (f) Ito, H.; Ikeda, M.; Hasegawa, T.; Furusho, Y.; Yashima, E. *J. Am. Chem. Soc.* **2011**, *133*, 3419–3432.

(7) (a) Barboiu, M.; Lehn, J. M. *Proc. Natl. Acad. Sci. U.S.A.* **2002**, *99*, 5201–5205. (b) Barboiu, M.; Vaughan, G.; Kyritsakas, N.; Lehn, J. M. *Chem.—Eur. J.* **2003**, *9*, 763–769.

(8) (a) Prest, P. J.; Prince, R. B.; Moore, J. S. *J. Am. Chem. Soc.* **1999**, *121*, 5933–5939. (b) Prince, R. B.; Saven, J. G.; Wolynes, P. G.; Moore, J. S. *J. Am. Chem. Soc.* **1999**, *121*, 3114–3121. (c) Prince, R. B.; Barnes, S. A.; Moore, J. S. *J. Am. Chem. Soc.* **2000**, *122*, 2758–2762. (d) Yang, W. Y.; Prince, R. B.; Sabelko, J.; Moore, J. S.; Gruebele, M. *J. Am. Chem. Soc.* **2000**, *122*, 3248–3249. (e) Prince, R. B.; Moore, J. S.; Brunsveld, L.; Meijer, E. W. *Chem.—Eur. J.* **2001**, *7*, 4150–4154. (f) Matsuda, K.; Stone, M. T.; Moore, J. S. *J. Am. Chem. Soc.* **2002**, *124*, 11836–11837. (g) Stone, M. T.; Heemstra, J. M.; Moore, J. S. *Acc. Chem. Res.* **2006**, *1*, 11–20. (h) Khan, A.; Kaiser, C.; Hecht, S. *Angew. Chem., Int. Ed.* **2006**, *45*, 1878–1881. (i) Zornik, D.; Meudtner, R. M.; Malah, T. E.; Thiele, C. M.; Hecht, S. *Chem.—Eur. J.* **2011**, *17*, 1473–1484. (j) Ticora, V. J.;

Morris, M. S.; Roberto, L.; Tom, F. A. G.; Gregory, N. T. *J. Am. Chem. Soc.* **2005**, *49*, 17235–17240.

(9) (a) Piguat, C.; Borkovec, M.; Hamacek, J.; Zeckert, K. *Coord. Chem. Rev.* **2005**, *249*, 705–726. (b) Albrecht, M. *Chem. Rev.* **2001**, *101*, 3457–3497.

(10) Since the distance between H₁ and H₂ (as shown in Figure 2) can be approximated as 2.47 Å, a relation between the integration of the observed cross-peaks and the distances can be determined (see the Supporting Information for more details).

(11) A dinuclear platinum(II) calix[4]arene bis-alkynyl complex containing two Pt-Bu₃trpy units has been reported to show Pt···Pt and π–π interactions in the solid state. See ref 3p.